ARTICLE OPEN

Check for updates

Parental high-fat/high-sugar diets and their lasting impact on brain development in offspring: a longitudinal mouse MRI study

Gail Lee[1,2,3]✉, Karina Wilk[4,5], Cheryl Chong[6], Jonas Yeung[1,2,3], Anne L. Wheeler[5,7], Jane A. Foster[8,9], Tie-yuan Zhang[10], Jason P. Lerch[1,3,5,11], Brian J. Nieman[1,2,3,12,15] and Mark R. Palmert[7,13,14,15]

Maternal diet and metabolic conditions, such as obesity and diabetes, are associated with consequences for offspring brain health, including effects on behaviour and an increased risk for neurodevelopmental disorders (NDDs). The extent and sequence of neuroanatomical changes to offspring brain development produced by dietary conditions have not yet been reported. In this study, we used a mouse model of parental high-fat or high-fat/high-sugar diet consumption to examine its effects on offspring brain development using longitudinal magnetic resonance imaging. We demonstrated that exposure to these parental diets through gestation and lactation resulted in offspring brain structure changes. Different temporal patterns of change were observed: some structures exhibited volume differences already at postnatal day 3; some of these early appearing changes diminished early in development while others were still present in adulthood; other structure changes were found to emerge later in the pubertal period. Brain changes in adulthood were present despite switching to a healthy diet at weaning. Brain regions impacted included the cingulate cortex, subregions of the hippocampus, and the orbitofrontal cortex, regions previously reported as affected in human NDD populations, with functional roles in reward processing and social cognition, memory, and decision making, respectively. Affected cortical regions, including the cingulate and orbitofrontal cortex, were found to be increased in volume relative to the whole brain, while affected subcortical regions were largely decreased in volume. Our data provide new insights into the long-term neuroanatomical impact of parental diets and how those diets may impact NDD risk. Future studies could use this model to evaluate preventative or ameliorative measures.

Translational Psychiatry (2025)15:500 ; https://doi.org/10.1038/s41398-025-03701-z

INTRODUCTION

Neurodevelopmental disorders (NDD) such as autism spectrum disorder and attention-deficit/hyperactivity disorder typically manifest early in development and impair cognitive and social functioning. Collectively, these conditions affect 4–18% of children [1, 2], with the reported prevalence varying widely depending on local diagnosis and screening practices, level of awareness, access to healthcare, and methodology or reporting [3]. While the cause of NDDs is undoubtedly multi-faceted [4], one consideration is the impact of early life environment on long-term brain development. Indeed, maternal obesity, gestational weight gain, and diabetes are associated with offspring brain health and NDD risk [5–8]. Since diet represents a common precursor to these metabolic conditions [9], understanding the impact of parental diet on offspring brain development is an important step to elucidating its potential role in NDD etiology. High-fat diets [10] and the "Western" diet, typified by the widespread consumption of ultra-processed and pre-packaged foods, high-sugar drinks, fried items, and high-fat dairy products [11], is one factor associated with increased prevalence of overweight and obesity [9], with 38% of the global population classified as being overweight or obese [12]. Thus, we elected to examine the impact on brain development of diets high in fat as well as high in fat and simple sugar (a combination selected to model key aspects of Western diet). Studying NDD etiology in relation to parental diet is a first step that could ultimately lead to efforts to promote healthier pregnancies and to develop interventions for offspring.

In practice, controlling and quantifying diet in humans is extremely challenging [13, 14]. It becomes even more difficult

[1]Mouse Imaging Centre, The Hospital for Sick Children, Toronto, ON, Canada. [2]Translational Medicine, The Hospital for Sick Children, Toronto, ON, Canada. [3]Department of Medical Biophysics, University of Toronto, Toronto, ON, Canada. [4]Department of Physics and Astronomy, University of Waterloo, Waterloo, ON, Canada. [5]Neuroscience and Mental Health, The Hospital for Sick Children, Toronto, ON, Canada. [6]Department of Biochemistry, University of Waterloo, Waterloo, ON, Canada. [7]Department of Physiology, The University of Toronto, Toronto, ON, Canada. [8]Department of Psychiatry and Behavioural Neurosciences, McMaster University, Hamilton, ON, Canada. [9]Center for Depression Research and Clinical Care, Department of Psychiatry, UT Southwestern Medical Center, Dallas, TX, USA. [10]Douglas Mental Health University Institute, Department of Psychiatry, McGill University, Montréal, QC, Canada. [11]Wellcome Centre for Integrative Neuroimaging, University of Oxford, Oxford, UK. [12]Ontario Institute for Cancer Research, Toronto, ON, Canada. [13]Department of Pediatrics, The University of Toronto, Toronto, ON, Canada. [14]Division of Endocrinology, The Hospital for Sick Children, Toronto, ON, Canada. [15]These authors contributed equally: Brian J. Nieman, Mark R. Palmert. ✉email: gailc.lee@alumni.utoronto.ca

Received: 2 December 2024 Revised: 12 September 2025 Accepted: 10 October 2025
Published online: 24 November 2025

when long timelines are required to study parental diet effects on offspring. Mouse models enable preclinical exploration of the link between parental diet consumption and offspring neurodevelopment in controlled environmental and genetic contexts. Indeed, models of high-fat diet consumption in C57BL/6 J mice recapitulate the metabolic characteristics of human conditions [15, 16]. Mice and humans also have largely homologous brain structure and comparable transcriptomic profiles [17]. While previous studies using mouse models of maternal high-fat diet consumption have demonstrated changes to the offspring brain morphology, signaling pathways, and behaviour [18–20], these findings have largely been reported in isolated brain regions or without the context of developmental trajectory. Our group recently exploited the high-throughput structural characterization possible with magnetic resonance imaging (MRI) to demonstrate that parental high-fat diet consumption in mice leads to widespread volume changes in the offspring brain in adulthood, including the extended amygdalar system which plays a role in reward-seeking behaviour [21]. However, this work was conducted at a single timepoint, and it is not yet known how parental diet affects offspring brain structure from birth through adulthood.

Therefore, in this study, our aim was to use longitudinal manganese-enhanced MRI (MEMRI) [22, 23] to establish the time course of offspring brain structure changes resulting from parental diet. Parent mice were fed one of three experimental diets starting in adolescence (P35) for an 8-week acclimation period and then throughout breeding, gestation, and lactation: a healthy rodent control diet (CD), a "Western" diet high in both fat and simple sugar (sucrose) (WD), or a high-fat diet without high sucrose (HFD). From weaning onwards, offspring from all groups were fed the CD, thus isolating the effect of parental and neonatal diet on long-term brain growth. MEMRI was performed in offspring at 8 different timepoints, spanning neonatal to adult ages, and the trajectory of neuroanatomical changes was quantified.

METHODS

Diets and animals

Five-week-old male and female C57BL/6 J mice were obtained from The Centre for Phenogenomics (TCP) in-house colony and kept on a 12 h light/dark cycle with access to food and water *ad libitum*. The mice were assigned groups in a block-randomized fashion (2-4 breeding pairs per block) and placed on one of the following diets: 1) the CD, consisting of 13% kcal from fat, 19% kcal from protein, 68% kcal from carbohydrates, and 12% weight from sucrose (TD.08485, Inotiv, formerly Envigo, IN, USA); 2) the WD, consisting of 42% kcal from fat, 15% kcal from protein, 43% kcal from carbohydrates, and 34% weight from sucrose (TD.88137, Inotiv, IN, USA); or 3) the HFD, consisting of 60% kcal from fat, 16% kcal from protein, 24% kcal from carbohydrates, and 12% weight from sucrose (TD.210337, Inotiv, IN, USA). Since the high fat content diets tended to crumble and fall from the standard food hoppers, the diet pellets were placed on the cage floor throughout the experimental time course for all diet groups. Due to evident visual differences in diets (colour and texture), investigators were not blinded to diet during experiments.

After an 8-week diet acclimation, diet-matched male and female mice were paired for mating for 4-6 days and then separated. Pregnant female mice were then singly housed and kept on their specified diet throughout gestation and lactation (Fig. 1A). Paw tattoos were applied on postnatal day (P)1 or P2 to uniquely identify offspring (AIMS NEO-9 Neonate Tattoo System, Animal Identification and Marking Systems, Inc., NY, USA). At three weeks of age (P21), all offspring mice were weaned onto CD, regardless of parental diet (CD, WD, or HFD). The mice used as parents to produce subject offspring were used for breeding only once, to keep a strict diet consumption period. Animal care and experimental procedures were approved by the TCP Animal Care Committee (AUP 25-0175H).

Body weights

Dam and sire weights were recorded weekly throughout the 8-week diet acclimation period. After the mice were paired for breeding, the following number of litters were produced for each diet type: n = 10 CD, 10 WD, and 11 HFD. Offspring mice were weighed before each MRI scan. The number of male (M) and female (F) offspring used for collection of experimental data were: n = 20 M/16 F CD, 18 M/14 F WD, and 20 M/16 F HFD. We aimed for a sample size of 15 mice per group per sex to provide sufficient power to capture ~3% volume change for main diet effects. Parental weight gain data was fit with a linear mixed-effects model using the lme4 package [24]. Fixed effects were included for age (treated categorically, with one for each of the 8 measurements), diet (categorical), and sex (categorical), along with their interactions. A random effect was included that allowed for a mouse-specific intercept. Offspring weights were normalized by the mean weight of CD offspring for each timepoint and sex. Then, the logarithm of normalized weights was fit with a linear mixed-effects model [24]. Fixed effects were included for diet (categorical) and sex (categorical), along with their interactions with age (treated categorically, with one for each of the timepoints). A random effect was included that allowed for a mouse-specific intercept. A p-value < 0.05 was considered statistically significant. Statistical analysis was performed using R (version 3.6.3) through Rstudio (2022.07.1 + 554) [25, 26]. The Satterthwaite approximation was used to estimate p-values using the lmerTest package [27].

In vivo longitudinal imaging

Magnetic resonance imaging. Longitudinal MRI of offspring was employed to characterize brain structure throughout development and into adulthood. To enhance neuroanatomical contrast, 0.4 mmol/kg dose of manganese (in the form of manganese chloride, $MnCl_2$) was administered intraperitoneally 24-h prior to scanning [28], either to the dam (up to offspring age P14) who passed the agent to offspring through maternal milk or directly to the offspring mice [23]. The mice were scanned using a multi-channel 7-Tesla 306-mm horizontal bore magnet (BioSpec 70/30 USR, Bruker, Ettlingen, Germany) with ParaVision 6.0.1 console software. This system is equipped with four cryogenically cooled radiofrequency coils [29] to allow simultaneous scanning of up to four mice [30, 31]. Brain images were obtained with a T1-weighted, 3D gradient echo sequence and the following parameters: $\alpha = 26°$, TR = 26 ms, TE = 8.25 ms, field-of-view = 25 × 22 × 22 mm, matrix size = 334 × 294 × 294, 2 repetitions, total acquisition time = 59 min, 75 µm isotropic resolution. The acquisition time was reduced by using a cylindrical k-space acquisition [32]. In most cases (~65%), the final image used for analysis consisted of the average of the two acquired repetitions. In the remaining cases, either a single repetition was judged to be of better quality or only a single repetition was acquired due to premature termination of the scan (either due to hardware failure or other issues).

Experimental time course. The number of pups in each litter was culled to a maximum of 6 to ensure balanced nutrients and care from the dams, as well as comparable manganese chloride uptake via maternal milk across the litters. A maximum of 2 male and 2 female pups were chosen from each litter for longitudinal scanning. Male and female offspring mice were scanned longitudinally across 8 postnatal timepoints: P3, P5, P7, P14, P28, P42, P65, and P150 (Fig. 1B). Scan timepoints were spaced more closely in the early postnatal period to capture the critical brain development occurring rapidly in early life, and then more sparsely continuing into adulthood. Females were not evaluated for estrous stage prior to imaging. After acquisition, images were evaluated for quality (signal-to-noise ratio, possible image artifact) and excluded if warranted (investigators were blinded during quality assessment). A total of 27 images were excluded due to poor image quality (6 images), poor segmentation at image registration (4 images), scans missed due to scanner downtime (4 images), mouse welfare concerns (9 images), or ambiguous paw tattoos at P3 (4 images). A total of 805 brain images were included in data analyses.

Image registration and analysis

All images were registered together through the Pydpiper toolkit [33], which utilizes the Advanced Normalization Tools (ANTs) [34] and the Montreal Neurological Institute (MNI) tools [35]. The longitudinal analysis employed a two-step process in which brain images were first aligned to an age-specific consensus average and then registered across different ages using a multi-level registration pipeline. This registration process was described in detail in Qiu et al., 2018 [23]. The MAGeT Brain algorithm [36] was used to automatically segment each of the 805 brain images into 182 bilateral brain regions using previously published atlases [37–40]. Using this algorithm, each image was first registered to the atlas. Then, within

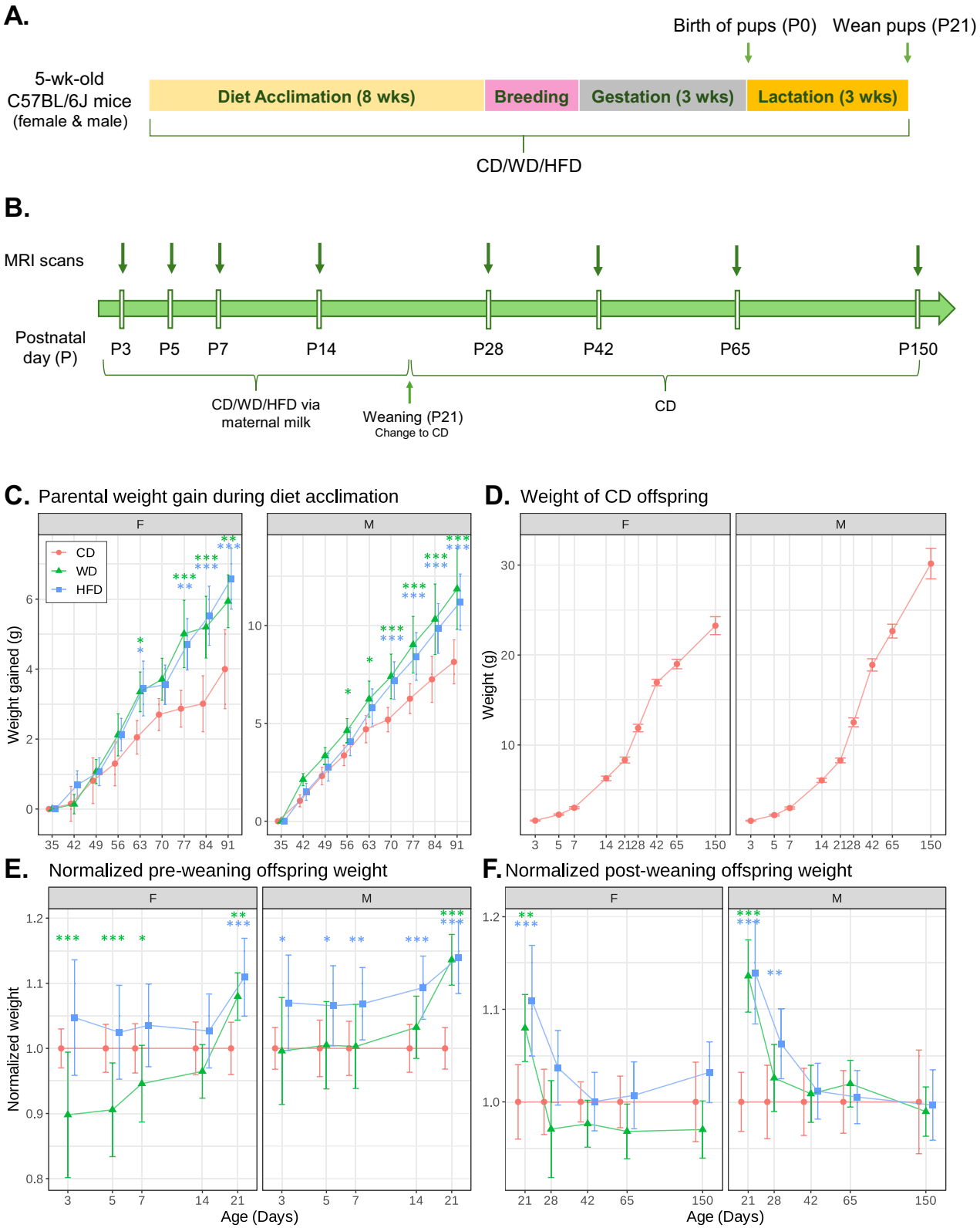

each scan timepoint, 25 images were randomly selected to be used as registration templates for the rest. Each individual image was then automatically segmented 25 times using the generated templates. In this work, the MAGeT algorithm was adjusted so that brain structure volumes for each individual image were determined by computing the median volume for each structure from the 25 candidate segmentations.

Relative brain structure volumes (i.e., normalized to whole brain volume) were fit with a piecewise linear mixed-effects (LME) model [24]. Fixed effects were included for age (treated categorically, with one coefficient for each of the 8 timepoints), diet (categorical, with five coefficients describing a piecewise linear change from CD), and sex (categorical, with five coefficients describing a piecewise linear change from female), along with

Fig. 1 Experimental timelines and weight measurements. A Timeline of parent mice diet acclimation, breeding, gestation, and lactation. Wk: week. P: postnatal day. **B** Timeline of offspring brain MRI scans, where the top green arrows indicate when the MRI scans were performed. **C** Mice began acclimation to experimental diets on postnatal day (P)35 and continued on those diets for 8 weeks prior to breeding. The average weight at P35 are as follows: females (18.8 g CD/17.9 g WD/17.9 g HFD) and males (22.2 g CD/22.4 g WD/22.3 g HFD). Number of mice represented are as follows: CD (10 M/10 F), WD (10 M/10 F), and HFD (11 M/11 F). **D** Weight gain trajectory of CD offspring mice. **E** Weights were normalized to the baseline CD group to show differences between diet groups. The average weight of CD male and female mice at P21 were 8.28 g and 8.32 g, respectively. Significant weight differences were seen at P21 in male and female offspring of WD group and HFD group. **F** The weight difference in offspring began to dissipate post weaning when they were all transitioned onto the CD. A logarithmic x-axis was used in panels D-F for a more equal spacing between the timepoints. All error bars represent 95% confidence intervals. The data points have been jittered horizontally for visualization purposes. F: female. M: male. Asterisks denote: *$p < 0.05$; **$p < 0.01$; ***$p < 0.001$ (based on a t-test of mixed model coefficients employing the Satterthwaite approximation for degrees of freedom).

all interactions. The five timepoint knots chosen for the diet and sex fixed effects were P3, P14, P28, P42, and P150, which represent neonatal, late postnatal, puberty, late adolescence, and later adulthood, respectively. A random effect was included that allowed for a mouse-specific intercept. Assessment of diet or diet-sex interaction effects was based on t-tests of the associated fixed effect coefficients in the model, employing the Satterthwaite approximation to estimate degrees of freedom. A false discovery rate (FDR) [41] threshold of 10% was used to correct statistics for multiple comparisons across all structures (i.e., a q-value < 0.1 was considered statistically significant). Normality and homoscedasticity of volume data were assessed for each structure using the Kolmogorov-Smirnov and Fligner-Killeen tests, respectively, and found to be valid (adjust p values > 0.99 and 0.17, respectively). Where total volume changes for a group of structures was evaluated (e.g., combined hippocampal CA3 region, total cingulate cortex, whole brain), the unadjusted p-values were used to assess significance.

To group structures that showed similar diet effects across the time course, a cluster analysis was conducted, as similarly done in Yeung et al. [42]. Structure-wise, relative volumes were first z-scored and then a vector was generated from the average values for each diet group at each timepoint, producing a matrix of 182 vectors each containing 24 values (3 diets, 8 timepoints). The distance between the vectors were calculated using the Euclidean method and hierarchical clustering was performed using the Ward D2 method [43]. The number of clusters retained was determined using an elbow plot.

The percent changes of brain structure volumes were calculated using the outputs of the LME model, by dividing the beta value of diet coefficients by the beta value of corresponding timepoint coefficients (i.e., the volume of the baseline control group at that timepoint) and multiplying by 100%. The 95% confidence intervals displayed in all scatter plots were generated from the raw data points (not from the model).

RESULTS

Parental WD or HFD consumption resulted in significant weight gain in dams, sires and offspring, but weight normalized in offspring after switch to CD at weaning

The body weight of parent mice was measured every week during the 8-week diet acclimation period to verify diet impact on parent physiology. Dams and sires fed either WD or HFD exhibited significantly greater weight gain compared to CD by the 5th week after diet introduction ($p < 0.05$, Fig. 1C). The average weight (reported as mean ± standard deviation) gained over the 8-week acclimation period are as follows: females (CD 4.0 ± 1.8 g; WD 5.9 ± 1.2 g; HFD 6.6 ± 1.5 g) and males (CD 8.1 ± 1.8 g; WD 11.9 ± 3.3 g; HFD 11.2 ± 2.4 g). In summary, WD dams gained 48.5% more weight than CD dams ($p < 0.01$), while HFD dams gained 64.5% more than CD dams ($p < 0.001$). Similarly, the WD and HFD sires respectively gained 45.8% and 37.6% more weight than CD sires ($p < 0.001$).

Both the male and female offspring of WD and HFD groups gained more weight pre-weaning and were heavier than CD offspring (Fig. 1D) at weaning (average weight difference at P21 vs CD offspring: +9% F, +14% M, $p < 0.01$; Fig. 1E). However, after offspring fed the WD and HFD were transitioned to the CD at weaning, the weight difference dissipated (average weight difference at P28 vs CD offspring: -1.2% F, +1.2% M, $p > 0.1$; Fig. 1F).

Diet manipulation in early life changed brain growth trajectories over offspring lifespan, including into adulthood

Offspring brains were imaged longitudinally from P3 to P150. Our primary analyses focused on relative brain volumes, calculated by normalizing individual structure volumes with whole-brain volume. The longitudinal time courses show many expected features, such as rapid volume growth and then volume decrease in cortical brain regions as well as slower initial but persistent growth of subcortical and white matter regions, resulting in a V-shape trajectory for many of these structures. Images revealed relative volume changes at all scan timepoints in animals exposed to WD and HFD during gestation and lactation (Fig. 2 and Supplementary Figure 1, which further separates by sex). The diets altered growth trajectories of different structures at varying developmental timepoints. Several structures showed transient changes in relative volumes in early postnatal development, either at P3 or through the period while still exposed to WD or HFD (20 and 30 structures, respectively). For example, the relative volume of the cerebral peduncle was smaller in WD and HFD compared to CD by P14 (-2.7% WD and -2.9% HFD, $q < 0.05$, Fig. 3A), but these differences waned slowly through development after switch to CD (-1.7% WD and -0.8% HFD, $q > 0.2$ at P28; -1.1% WD and -0.6% HFD, $q > 0.3$ at P150). Other structures displayed a different pattern with early structural changes that were conserved in the later timepoints (i.e., P42 or P150), well after transitioning to CD at weaning (P21) and despite the normalization of diet-induced weight differences observed in the pre-weaning period. One example of this pattern is increased cingulate cortex volume observed in both WD and HFD offspring at P3 and P150 (+ 1.2% WD and +2.0% HFD, $p < 0.05$ at P3; +3.0% WD and +3.0% HFD, $p < 1 \times 10^4$ at P150; Fig. 3B). In total, 7 and 13 structures in WD and HFD, respectively, displayed these early differences (pre-weaning) which were also significant in adulthood. Lastly, a larger number of structures (40 and 27 structures in WD and HFD, respectively) followed a different trajectory with alterations that emerged after weaning and into adulthood, as seen in the habenular commissure (+2.4% WD and +1.0% HFD, $q > 0.9$ at P3; -17.9% WD and -11.3% HFD, $q < 0.1$ at P28; -12.9% WD and -11.7% HFD, $q < 1 \times 10^4$ at P150; Fig. 3C) and hippocampal CA3 region (-0.8% WD and +0.5% HFD, $p > 0.1$ at P3; -1.7% WD and -2.0% HFD, $p < 0.05$ at P28; -2.2% WD and -2.5% HFD, $p < 0.001$ at P150; Fig. 3D). Percent volume changes for all 182 structures at each of the 5 timepoint knots of the LME model are listed in Supplementary Table 1. It is intriguing that many of the structures with observed volume changes in our study have also been reported to have structural changes in human NDDs. A listing of structures identified here with corresponding examples of human findings is provided in Supplementary Table 2, though we emphasize that such correspondence is exploratory and must be interpreted cautiously.

Since we observed the different developmental patterns noted above, we sought not only to identify individual structures evidencing developmental differences but also to group structures in the whole brain based on consistent patterns of change over time and across diets. To do this, we conducted a cluster

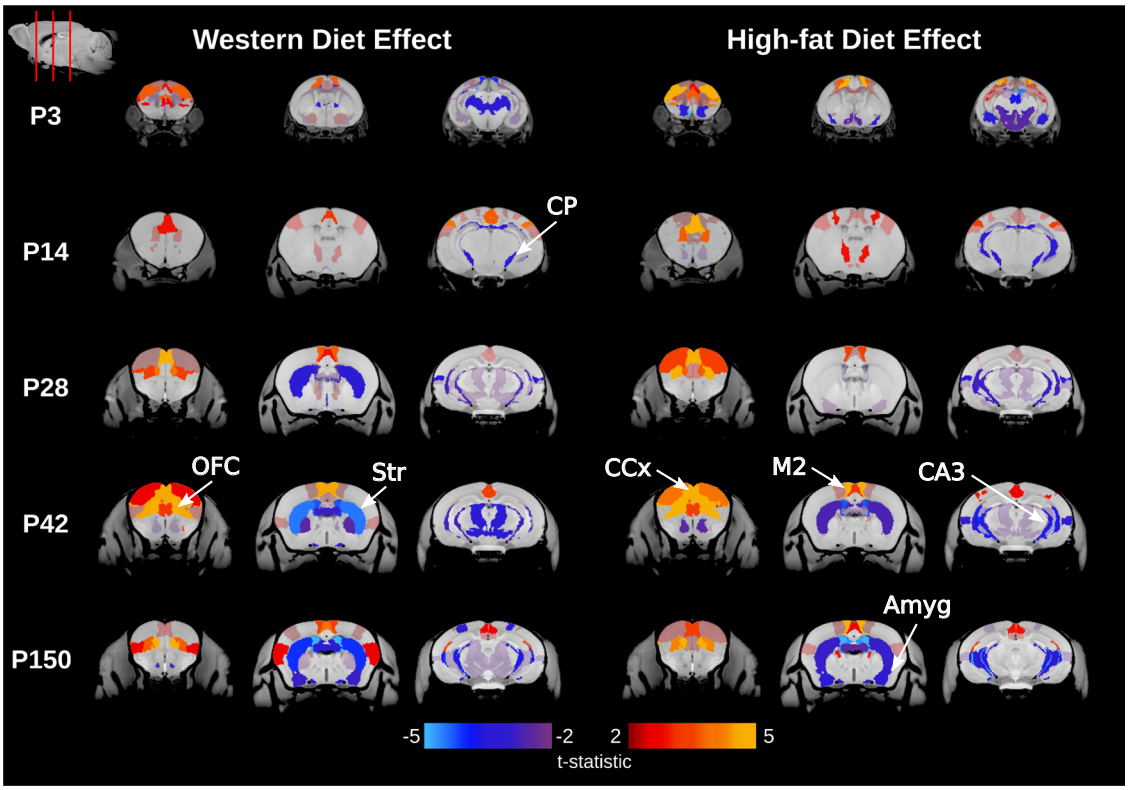

Fig. 2 Sample neuroanatomical structures whose relative volumes were affected by diet through development. Gestational and early-life consumption of WD or HFD was found to affect the relative volume of several brain structures from neonatal period (P3) to adulthood (P150). Each column follows a coronal cross-section of the developing brain through the experimental timepoints down the rows. Warm colours indicate structures relatively larger in experimental diet groups and cool colours indicate structures relatively smaller in experimental diet groups. Opaque colours represent significant structures after multiple comparisons correction across both diets at 10% FDR, applied at each timepoint. Transparent colours represent structures with uncorrected p-value of less than 0.05, computed based on a t-test of mixed model coefficients employing the Satterthwaite approximation for degrees of freedom. T-values greater than 5 or less than -5 were clamped by the colour bar for display purposes. The slice indicator on the top left corner shows the location of the coronal cross-section slices. CP: cerebral peduncle. OFC: orbitofrontal cortex. Str: striatum. CCx: cingulate cortex. M2: secondary motor cortex. CA3: hippocampal CA3 region. Amyg: amygdala.

analysis (Fig. 4A) based on 6 clusters, a number selected based on an elbow plot of residual variance versus cluster number (Supplementary Figure 2). The relative volumes of structures belonging to each of the 6 clusters were summed for each mouse and averaged to visualize cluster patterns by diet across time (Fig. 4B-G). Clusters 1 and 5 exhibited decreased volumes in WD and HFD groups. Cluster 1 consisted of subcortical structures, including the amygdala, nucleus accumbens, and colliculi, whereas cluster 5 included the hippocampal CA3 region and some cortical structures (e.g., primary visual cortex and perirhinal cortex). Clusters 3 and 6 exhibited a different pattern with increased volumes in WD and HFD groups, with both comprised primarily of cortical structures (25 of 46 and 16 of 22 structures by count, respectively). However, the structures belonging to cluster 3 predominantly included regions in the cingulate and temporal cortices, whose relative volumes were collectively larger in WD and HFD offspring during the post-weaning and adult period, whereas those belonging to cluster 6 predominantly included regions in the cingulate and frontal cortices, whose relative volumes were collectively larger in WD and HFD offspring throughout development from early postnatal period. Clusters 2 and 4 exhibited minimal impacts of perinatal diet, with differences seen in early postnatal periods which disappeared through development.

We also explored sex and diet-sex interaction effects on individual structures. As expected, we observed increased relative volumes of the medial amygdala (+13.7%, $q < 10^{-13}$ at P150; Supplementary Figure 3A) and bed nucleus of stria terminalis (+5.6%, $q < 0.01$ at P150; Supplementary Figure 3B) in males compared to females, which emerged post-weaning and were observed regardless of diet exposure. There were 50 other structures ($q < 0.1$) that showed significant sex effects at different stages through development (Supplementary Figure 3C). There were also several structures (32 total, $q < 0.1$) that showed small but statistically significant diet-sex interaction effects. These effects were significant mainly at the early neonatal timepoint (P3). The hypothalamus in WD males showed a significant volume offset from WD females at P3 but the difference disappeared by P14 (diet-sex interaction effect: -3.0%, $q < 0.01$ at P3; -1.1%, $q > 0.9$ at P14; Fig. 3E).

Overall, WD and HFD affected a similar profile of structures and with a similar direction of change. However, some diet differences were noted. When HFD offspring brains were compared with WD offspring brains, significant differences were found in 42 structures ($q < 0.1$). Most of these WD-HFD differences were present at P3 timepoint and disappeared by the second week of postnatal life (Supplementary Figure 4). For example, the corpus callosum had a larger relative volume in HFD offspring than WD offspring at P3 (+ 2.5% in HFD vs WD, $q < 0.1$), and this difference was absent by P14 (-0.8%, $q = 1.0$; Fig. 3F).

While we focus here on relative brain volume data, we did also conduct analyses of absolute brain volumes (please refer to the Supplementary Materials for detailed methods and results; see Supplementary Figure 5).

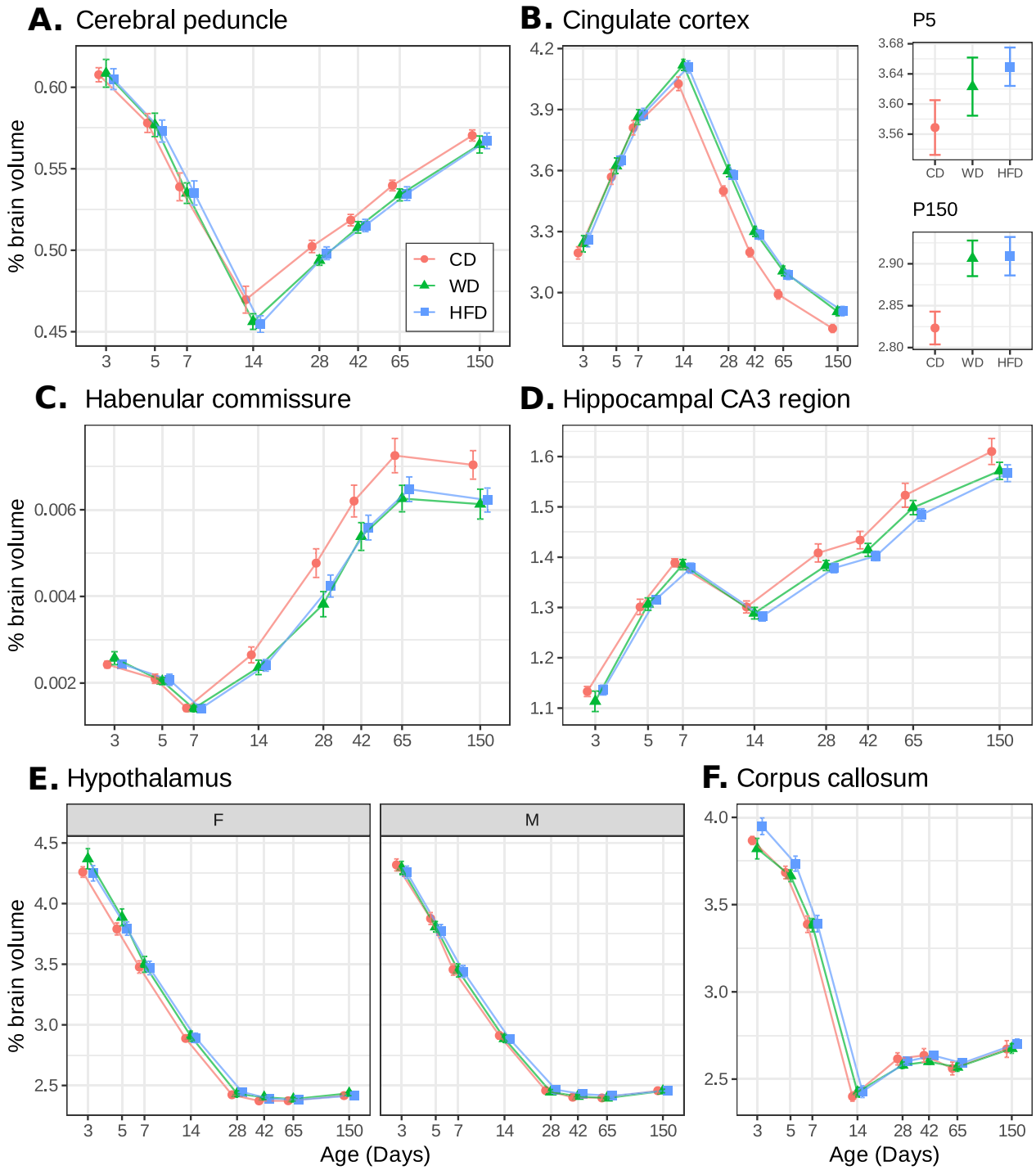

Fig. 3 Diets induced different trajectories of brain structure development in relative volume. (**A**) The cerebral peduncle relative volume was significantly affected by both WD and HFD at late postnatal period (P14), but this difference disappeared post weaning. **B** The cingulate cortex relative volume was increased in WD and HFD offspring from neonatal development (P3) and persisting into later adulthood (P150). The diet effect on (**C**) the habenular commissure and **(D)** the hippocampal CA3 region emerged in the pubertal period (P28) and persisted through development. (**E**) WD effect on the hypothalamus at P3 was different based on offspring sex. (**F**) The corpus callosum relative volume was significantly larger in HFD offspring compared to WD offspring at neonatal timepoint (P3) but this appeared to be only transient. Number of mice represented are as follows: CD (20 M/16 F), WD (18 M/14 F), and HFD (20 M/16 F). A logarithmic x-axis was used in all the panels for a more equal spacing between the timepoints. All error bars represent 95% confidence intervals. The data points have been jittered horizontally for visualization purposes.

DISCUSSION

Our data demonstrate that exposure to high-fat or high-fat/high-sugar (i.e., WD) parental diet during gestation and lactation has small but long-lasting effects on offspring brain structure, with impact still seen well into adulthood. Exposure to the WD or HFD over an 8-week period induced significant weight gain in parent mice, consistent with previous literature [21, 44]. The dams were maintained on these diets throughout gestation and lactation, and this exposure resulted in

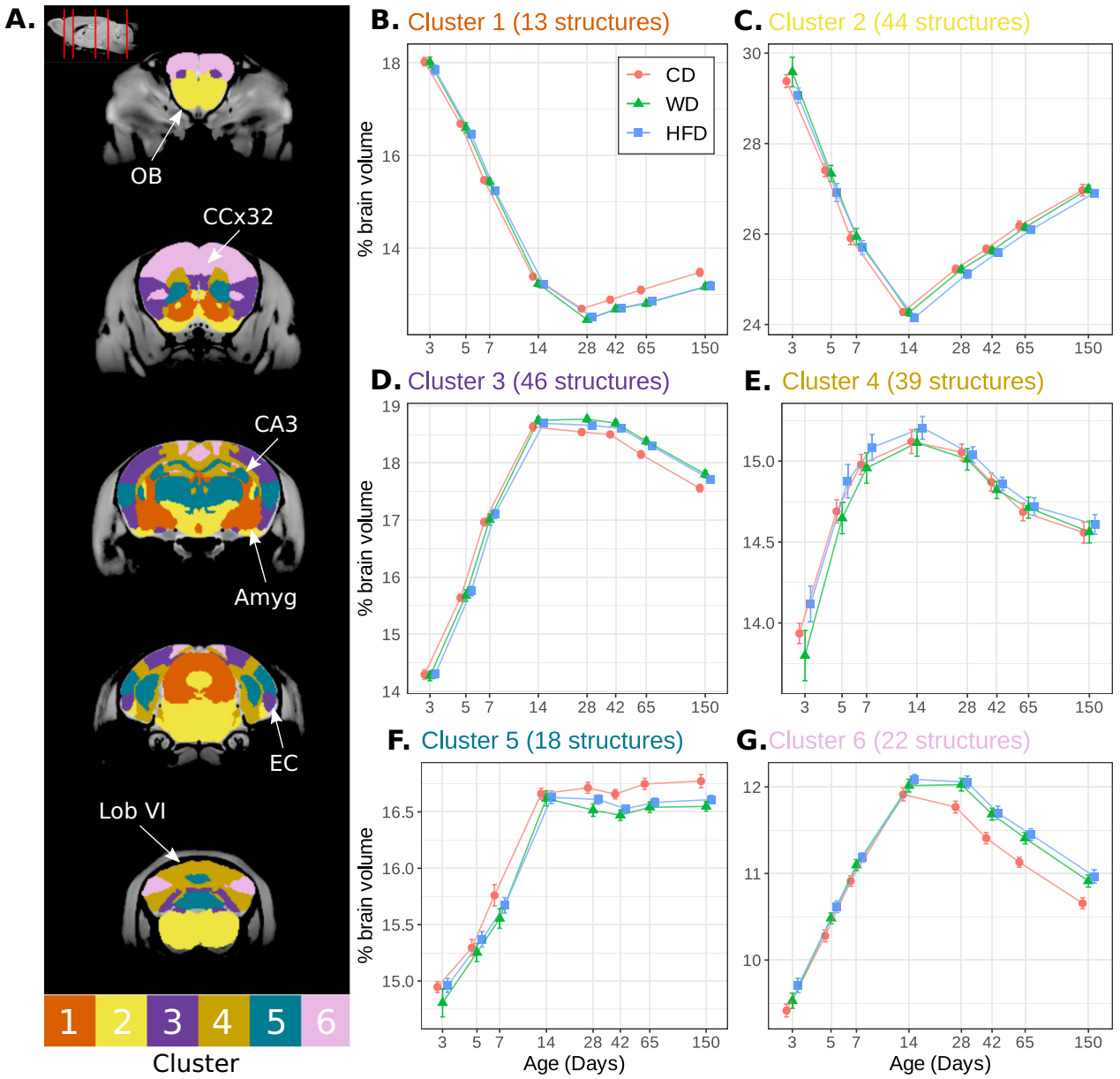

Fig. 4 Clusters of structure relative volume change. A The structures were grouped into 6 clusters based on their pattern of relative volume change through development and additional impact of perinatal diet exposure. The slice indicator on the top left corner shows the location of the coronal cross-section slices. OB: olfactory blub. CCx32: cingulate cortex area 32. CA3: hippocampal CA3 region. Amyg: amygdala. EC: entorhinal cortex. Lob VI: cerebellar lobule VI. **B** Cluster 1 consisted of subcortical structures whose relative volumes were collectively smaller in WD and HFD offspring than CD offspring, mainly post weaning and into adulthood. **C** Cluster 2 consisted of subcortical structures with minimal diet effects at pre weaning period. **D** Cluster 3 consisted of mainly cortical structures, whose relative volumes were collectively larger in WD and HFD offspring from post weaning period and onwards. **E** Cluster 4 consisted of mainly cortical structures with varying diet effects restricted to pre weaning period. **F** Cluster 5 consisted of hippocampal and cortical structures whose relative volumes were collectively smaller in WD and HFD offspring, mostly post weaning and into adulthood. **G** Cluster 6 consisted of mainly cortical structures, whose relative volumes were collectively larger in WD and HFD offspring throughout the entire developmental trajectory. A logarithmic x-axis was used in panels B-G for a more equal spacing between the timepoints. All error bars represent 95% confidence intervals. The data points have been jittered horizontally for visualization purposes.

heavier offspring than those produced by CD-fed parents, though weights then normalized over time once offspring were transitioned to the control diet [21, 45]. Similarly, an observational study in humans has also revealed that maternal pro-inflammatory diet consumption during pregnancy led to increased offspring body mass index and growth rate in childhood [46]. Consistent with previous findings [21], we observed offspring brain structure changes into adulthood despite early transition to a healthy diet and weight normalization. Our data showed that structures involved in reward processing were impacted in adulthood by parental diet, similar to findings reported by Fernandes et al. [21]. We note, however, that the Fernandes study showed a wider extent of brain regions impacted, which we attribute primarily to differences in the specific diets used. The persistence of offspring brain changes into adulthood due to parental and early life diet evokes the broader theory of developmental origins of health and disease, which hypothesizes that early-life environmental exposures permanently influence health throughout the lifespan [47, 48].

This study is novel in that we followed offspring brain development longitudinally with MRI from birth to adulthood with the aim of further defining the impact of perinatal diet exposure. The time course of structure volume change has potential translational implications. For example, we found that many structures exhibited a volume change that emerged in the late postnatal or peripubertal period. For these structures, one wonders whether there is an early window of opportunity for postnatal interventions in offspring to prevent/ameliorate some of these changes. For example, future studies could explore exercise or omega-3 fatty acid supplementation – reported to modulate aspects of behaviour in NDDs and obesity-induced neuroinflammation, respectively [49, 50] – as a strategy to mitigate structural changes even after exposure to parental/early-life diet. Prevention or remediation of the structural changes that we observe in the early neonatal period (i.e., at P3), which correspond to late gestational timepoints in humans, may require earlier intervention, prior to birth [51]. In the context of our mouse study, it would be interesting to also investigate maternal care behaviour. Different diets might lead to changes in nursing, nesting or other care behaviours that could influence subsequent offspring neurodevelopment. Such differences, if also a factor for humans, could also represent modifiable risks for brain development in newborns [52].

In our analyses, we focused primarily on relative structure volumes, which account for whole brain volume differences. Generally, this accounts for biological variability and is more sensitive to small regional changes or in circumstances with a high degree of variability, such as seen in younger mice [23, 53]. Many of the structures with observed changes at multiple developmental timepoints in our data have previously been reported to be altered in human NDD populations (Supplementary Table 2). A few notable structures included the cingulate cortex [54–56], hippocampus [55], and prefrontal cortex [54, 55], which together play an important role in emotion, reward processing, social cognition, decision making, and cognition [57–59]. Children with NDDs have impairments of these functions, such as aberrant reward processing [60] and emotional dysregulation [61] in ADHD, social impairments in ASD [62], decision making deficits [63] in ID, and cognitive deficits in ASD [64], ADHD [65], and ID [62]. Volumetric changes in these brain structures may suggest underlying cellular changes that contribute to the reported functional deficits.

Interestingly, most of the structures with increased relative volume (e.g. cingulate cortex, orbitofrontal cortex, secondary motor cortex, primary somatosensory cortex) in adult WD or HFD offspring were cortical regions, whereas the structures with decreased volume (e.g. hippocampal CA3 region, striatum) were subcortical regions. Larger cortical volumes may indicate an abnormality in the typical pattern of cortical thinning during development, which is a feature previously reported in the ASD population [66, 67]. However, there has also been a report of decreased cortical thickness in human ASD population, particularly in the temporal lobe [68], as well as decreased cortical volume in adult mice with diet-induced obesity, where the authors suggested a likely involvement of microglia dysregulation [69]. A slightly reduced volume of the whole brain as well as a greater volume reduction of subcortical structures have been reported in the ADHD populations, where caudate, putamen, and thalamus were found to be disproportionately smaller [70]. These relationships require further study and may provide insights into how parental diet [71] – and possibly obesity and other maternal metabolic abnormalities – may increase offspring NDD risk in humans.

Our relative volume findings demonstrate that the effects of WD and HFD on offspring brain structure were largely similar, especially later in development and into adulthood. We hypothesize that this similarity indicates the fat component of the diets has more long-lasting effect on offspring than the sugar component, as a high fat component was a shared feature of the two experimental diets. The mechanism of the diet-induced changes is not clear but may stem from the metabolic environment and inflammation. It has been shown that obese pregnant mice have increased levels of circulating insulin, leptin, and cholesterol during late gestation [72], and maternal obesity may also be accompanied by hyperglycemia [73]. Hence, the offspring are exposed to increased levels of circulating nutrients (e.g. glucose) and metabolic hormones (e.g. leptin, insulin), which can also be passed onto the fetal circulation [74]. Appropriate levels of nutrients and hormones are necessary for proper brain development and maturation, and their excess or deficit may disrupt normal developmental processes [75, 76]. Additionally, obesity produces a state of low-grade chronic inflammation, because the increase in adipose tissue mass leads to increased secretion of inflammatory cytokines, such as interleukin-6 (IL-6), interleukin-1β, and tumor necrosis factor-α (TNF-α) [77]. Studies using a mouse model of HFD-induced maternal obesity found elevated IL-6 levels in the maternal serum [78, 79] and the placenta [79] at late gestation, along with an increase in cytokine levels in fetal circulation [79]. Pro-inflammatory cytokines may result in direct injury to neurons and oligodendrocytes or act indirectly through microglial activation, which can damage surrounding cells with the secretion of pro-inflammatory cytokines and free radicals [80]. The disruption of early brain development due to inflammatory processes could result in long-lasting consequences as observed in this study.

Our studies have utilized a mouse model to allow us to study impact of diet while holding other variables constant. Further study of the model could explore the influence of age at time of parental diet exposure as well as age at pregnancy to determine how these might modulate diet impact on the brain. It would also be of interest in future studies to investigate how controlled dietary exposures, as demonstrated here, affect brain structure development in different contexts, as other lifestyle factors, environmental exposures, underlying genomic variations, and their interactions also contribute to NDD development [81]. Future mouse studies could also assess parental diet as an added risk factor in the context of genetic mouse models of NDDs, allowing such interactions to be probed experimentally without the confounding variability inherent in human studies. For example, a post-weaning HFD exposure altered dopamine signaling in the BTBR mouse model of ASD and elevated inflammatory processes in the *Cc2d1a* conditional knockout mouse model of ASD, resulting in exacerbation of behavioral abnormalities [82, 83]. Gestational and neonatal dietary exposures and neurodevelopmental brain structure changes in these contexts would be valuable to further our understanding of the mechanistic associations with NDD risk. It would also provide an experimental setting to investigate possible interventions [79].

In summary, we utilized MRI in a mouse model of parental diet exposures to enhance our understanding of how early-life diet affects offspring neurodevelopment from birth to adulthood. The effects of diet during gestation and lactation on offspring brain structure emerged early and were long-lasting, even after transitioning to a healthy control diet at weaning. Many brain structures, including both cortical and subcortical regions, showed different trajectories of volume change after perinatal diet exposure, some of which overlap with brain differences previously reported in human NDD populations. Since diet represents a modifiable risk factor for NDDs in humans, these findings highlight the importance of dietary considerations gestationally and provide a means of exploring intervention experimentally.

DATA AVAILABILITY

All software used to perform the analysis is open-source. Code and data are available upon reasonable request.

CODE AVAILABILITY

All software used to perform the analysis is open-source. Code and data are available upon reasonable request.

REFERENCES

1. Zablotsky B, Black LI, Maenner MJ, Schieve LA, Danielson ML, Bitsko RH, et al. Prevalence and trends of developmental disabilities among children in the United States: 2009–2017. Pediatrics. 2019;144:e20190811.
2. Miller AR, Mâsse LC, Shen J, Schiariti V, Roxborough L. Diagnostic status, functional status and complexity among Canadian children with neurodevelopmental disorders and disabilities: a population-based study. Disabil Rehabil. 2013;35:468–78.
3. Francés L, Quintero J, Fernández A, Ruiz A, Caules J, Fillon G, et al. Current state of knowledge on the prevalence of neurodevelopmental disorders in childhood according to the DSM-5: a systematic review in accordance with the PRISMA criteria. Child Adolesc Psychiatry Ment Health. 2022;16:27.
4. Bourgeron T. in *What Do We Know about Early Onset Neurodevelopmental Disorders? Translational Neuroscience: Toward New Therapies*. (eds. Nikolich, K. & Hyman, S. E.)(MIT Press, Cambridge (MA), 2015). 671–48.
5. Li M, Fallin MD, Riley A, Landa R, Walker SO, Silverstein M, et al. The association of maternal obesity and diabetes with autism and other developmental disabilities. Pediatrics. 2016;137:e20152206.
6. Kong L, Chen X, Gissler M, Lavebratt C. Relationship of prenatal maternal obesity and diabetes to offspring neurodevelopmental and psychiatric disorders: a narrative review. Int J Obes (Lond). 2020;44:1981–2000.
7. Norr ME, Hect JL, Lenniger CJ, Van den Heuvel M, Thomason ME. An examination of maternal prenatal BMI and human fetal brain development. J Child Psychol Psychiatry. 2021;62:458–69.
8. Wu D, Li Y, Chen L, Klein M, Franke B, Chen J, et al. Maternal gestational weight gain and offspring's neurodevelopmental outcomes: A systematic review and meta-analysis. Neuroscience Biobehav Rev. 2023;153:105360.
9. Wang L, Wang H, Zhang B, Popkin BM, Du S. Elevated fat intake increases body weight and the risk of overweight and obesity among chinese adults: 1991–2015 trends. Nutrients. 2020;12:3272.
10. Mazza E, Troiano E, Ferro Y, Lisso F, Tosi M, Turco E, et al. Obesity, dietary patterns, and hormonal balance modulation: gender-specific impacts. Nutrients. 2024;16:1629.
11. Clemente-Suárez VJ, Beltrán-Velasco AI, Redondo-Flórez L, Martín-Rodríguez A, Tornero-Aguilera JF. Global impacts of western diet and its effects on metabolism and health: a narrative review. Nutrients. 2023;15:2749.
12. Lobstein T, Jackson-Leach R, Powis J, Brinsden H & Gray M. World Obesity Atlas 2023. (2023)
13. Caut C, Leach M, Steel A. Dietary guideline adherence during preconception and pregnancy: A systematic review. Matern Child Nutr. 2020;16:e12916.
14. Crichton GE, Howe PRC, Buckley JD, Coates AM, Murphy KJ, Bryan J. Long-term dietary intervention trials: critical issues and challenges. Trials. 2012;13:111.
15. Surwit RS, Feinglos MN, Rodin J, Sutherland A, Petro AE, Opara EC, et al. Differential effects of fat and sucrose on the development of obesity and diabetes in C57BL/6J and A/J mice. Metabolism. 1995;44:645–51.
16. Rossmeisl M, Rim JS, Koza RA, Kozak LP. Variation in type 2 diabetes-related traits in mouse strains susceptible to diet-induced obesity. Diabetes. 2003;52:1958–66.
17. Beauchamp A, Yee Y, Darwin BC, Raznahan A, Mars RB, Lerch JP. Whole-brain comparison of rodent and human brains using spatial transcriptomics. eLife. 2022;11:e79418.
18. Buffington SA, Di Prisco GV, Auchtung TA, Ajami NJ, Petrosino JF, Costa-Mattioli M. Microbial reconstitution reverses maternal diet-induced social and synaptic deficits in offspring. Cell. 2016;165:1762–75.
19. Cruz-Carrillo G, Trujillo-Villarreal LA, Ángeles-Valdez D, Concha L, Garza-Villarreal EA, Camacho-Morales A. Prenatal cafeteria diet primes anxiety-like behavior associated to defects in volume and diffusion in the fimbria-fornix of mice offspring. Neuroscience. 2023;511:70–85.
20. Xu Y, Yang D, Wang L, Król E, Mazidi M, Li L, et al. Maternal high fat diet in lactation impacts hypothalamic neurogenesis and neurotrophic development, leading to later life susceptibility to obesity in male but not female mice. Adv Sci (Weinh). 2023;10:e2305472.
21. Fernandes DJ, Spring S, Roy AR, Qiu LR, Yee Y, Nieman BJ, et al. Exposure to maternal high-fat diet induces extensive changes in the brain of adult offspring. Transl Psychiatry. 2021;11:149.
22. Malheiros JM, Paiva FF, Longo BM, Hamani C, Covolan L. Manganese-enhanced MRI: biological applications in neuroscience. Front Neurol. 2015;6:161.
23. Qiu LR, Fernandes DJ, Szulc-Lerch KU, Dazai J, Nieman BJ, Turnbull DH, et al. Mouse MRI shows brain areas relatively larger in males emerge before those larger in females. Nat Commun. 2018;9:2615.
24. Bates D, Mächler M, Bolker B, Walker S. Fitting linear mixed-effects models using lme4. J Stat Soft. 2015;67:1–48.
25. R Core Team. R: A language and enviornment for statistical computing. (2020)
26. RStudio Team. RStudio: Integrated Development for R. RStudio, PBC (2020)
27. Kuznetsova A, Brockhoff PB, Christensen RHB. Lmertest package: tests in linear mixed effects models. J Stat Soft. 2017;82:1–26.
28. Aoki I, Wu Y-JL, Silva AC, Lynch RM, Koretsky AP. In vivo detection of neuroarchitecture in the rodent brain using manganese-enhanced MRI. NeuroImage. 2004;22:1046–59.
29. Arbabi A, Spencer Noakes L, Vousden D, Dazai J, Spring S, Botelho O, et al. Multiple-mouse magnetic resonance imaging with cryogenic radiofrequency probes for evaluation of brain development. NeuroImage. 2022;252:119008.
30. Bock NA, Konyer NB, Henkelman RM. Multiple-mouse MRI. Magn Reson Med. 2003;49:158–67.
31. Bock NA, Nieman BJ, Bishop JB, Mark Henkelman R. In vivo multiple-mouse MRI at 7 Tesla. Magn Reson Med. 2005;54:1311–6.
32. Spencer Noakes TL, Henkelman RM, Nieman BJ. Partitioning k-space for cylindrical three-dimensional rapid acquisition with relaxation enhancement imaging in the mouse brain. NMR Biomed. 2017;30:e3802.
33. Friedel M, Van Eede MC, Pipitone J, Chakravarty MM, Lerch JP. Pydpiper: a flexible toolkit for constructing novel registration pipelines. Front Neuroinform. 2014;8:1–21.
34. Avants B, Tustison NJ, Song G. Advanced Normalization Tools: V1.0. The Insight Journal. 2009;2:1–35.
35. Collins DL, Neelin P, Peters TM, Evans AC. Automatic 3D intersubject registration of MR volumetric data in standardized talairach space. J Comput Assist Tomogr. 1994;18:192–205.
36. Chakravarty MM, Steadman P, Van Eede MC, Calcott RD, Gu V, Shaw P, et al. Performing label-fusion-based segmentation using multiple automatically generated templates: MAGeT brain: label fusion segmentation using automatically generated templates. Hum Brain Mapp. 2013;34:2635–54.
37. Dorr AE, Lerch JP, Spring S, Kabani N, Henkelman RM. High resolution three-dimensional brain atlas using an average magnetic resonance image of 40 adult C57Bl/6J mice. NeuroImage. 2008;42:60–9.
38. Steadman PE, Ellegood J, Szulc KU, Turnbull DH, Joyner AL, Henkelman RM, et al. Genetic effects on cerebellar structure across mouse models of autism using a magnetic resonance imaging atlas. Autism Res. 2014;7:124–37.
39. Ullmann JFP, Watson C, Janke AL, Kurniawan ND, Reutens DC. A segmentation protocol and MRI atlas of the C57BL/6J mouse neocortex. NeuroImage. 2013;78:196–203.
40. Richards K, Watson C, Buckley RF, Kurniawan ND, Yang Z, Keller MD, et al. Segmentation of the mouse hippocampal formation in magnetic resonance images. NeuroImage. 2011;58:732–40.
41. Genovese CR, Lazar NA, Nichols T. Thresholding of statistical maps in functional neuroimaging using the false discovery rate. NeuroImage. 2002;15:870–8.
42. Yeung J, DeYoung T, Spring S, De Guzman AE, Elder MW, Beauchamp A, et al. Sex chromosomes and hormones independently influence healthy brain development but act similarly after cranial radiation. Proc Natl Acad Sci USA. 2024;121:e2404042121.
43. Murtagh F, Legendre P. Ward's hierarchical agglomerative clustering method: which algorithms implement ward's criterion?. J Classif. 2014;31:274–95.
44. Caprioli B, Eichler RAS, Silva RNO, Martucci LF, Reckziegel P, Ferro ES. Neurolysin knockout mice in a diet-induced obesity model. Int J Mol Sci. 2023;24:15190.
45. Saengnipanthkul S, Noh HL, Friedline RH, Suk S, Choi S, Acosta NK, et al. Maternal exposure to high-fat diet during pregnancy and lactation predisposes normal weight offspring mice to develop hepatic inflammation and insulin resistance. Physiol Rep. 2021;9:e14811.
46. Monthé-Drèze C, Rifas-Shiman SL, Aris IM, Shivappa N, Hebert JR, Sen S, et al. Maternal diet in pregnancy is associated with differences in child body mass index trajectories from birth to adolescence. Am J Clin Nutr. 2021;113:895–904.
47. Marshall NE, Abrams B, Barbour LA, Catalano P, Christian P, Friedman JE, et al. The importance of nutrition in pregnancy and lactation: lifelong consequences. Am J Obstet Gynecol. 2022;226:607–32.
48. Heindel JJ, Vandenberg LN. Developmental origins of health and disease: a paradigm for understanding disease cause and prevention. Curr Opin Pediatr. 2015;27:248–53.
49. Sun W, Yu M, Zhou X. Effects of physical exercise on attention deficit and other major symptoms in children with ADHD: A meta-analysis. Psychiatry Res. 2022;311:114509.
50. De Mello AH, Schraiber RDB, Goldim MPDS, Garcez ML, Gomes ML, De Bem Silveira G, et al. Omega-3 fatty acids attenuate brain alterations in high-fat diet-induced obesity model. Mol Neurobiol. 2019;56:513–24.
51. Na X, Raja R, Phelan NE, Tadros MR, Moore A, Wu Z, et al. Mother's physical activity during pregnancy and newborn's brain cortical development. Front Hum Neurosci. 2022;16:943341.

52. Lee A, Poh JS, Wen DJ, Tan HM, Chong Y-S, Tan KH, et al. Maternal care in infancy and the course of limbic development. Dev Cogn Neurosci. 2019;40:100714.
53. Lerch JP, Gazdzinski L, Germann J, Sled JG, Henkelman RM, Nieman BJ. Wanted dead or alive? The tradeoff between in-vivo versus ex-vivo MR brain imaging in the mouse. Front Neuroinform. 2012;6:6.
54. Guo Z, Tang X, Xiao S, Yan H, Sun S, Yang Z, et al. Systematic review and meta-analysis: multimodal functional and anatomical neural alterations in autism spectrum disorder. Mol Autism. 2024;15:16.
55. Connaughton M, O'Hanlon E, Silk TJ, Paterson J, O'Neill A, Anderson V, et al. The limbic system in children and adolescents with attention-deficit/hyperactivity disorder: a longitudinal structural magnetic resonance imaging analysis. Biol Psychiatry Glob Open Sci. 2024;4:385–93.
56. Mannerkoski MK, Heiskala HJ, Van Leemput K, Aberg LE, Raininko R, Hämäläinen J, et al. Subjects with intellectual disability and familial need for full-time special education show regional brain alterations: a voxel-based morphometry study. Pediatr Res. 2009;66:306–11.
57. Rolls ET. The cingulate cortex and limbic systems for emotion, action, and memory. Brain Struct Funct. 2019;224:3001–18.
58. Tulving E, Markowitsch HJ. Episodic and declarative memory: role of the hippocampus. Hippocampus. 1998;8:198–204.
59. Euston DR, Gruber AJ, McNaughton BL. The role of medial prefrontal cortex in memory and decision making. Neuron. 2012;76:1057–70.
60. von Rhein D, Cools R, Zwiers MP, van der Schaaf M, Franke B, Luman M, et al. Increased neural responses to reward in adolescents and young adults with attention-deficit/hyperactivity disorder and their unaffected siblings. J Am Acad Child Adolesc Psychiatry. 2015;54:394–402.
61. Vetter NC, Buse J, Backhausen LL, Rubia K, Smolka MN, Roessner V. Anterior insula hyperactivation in ADHD when faced with distracting negative stimuli. Hum Brain Mapp. 2018;39:2972–86.
62. American Psychiatric Association. *Diagnostic and Statistical Manual of Mental Disorders: DSM-5*. (American psychiatric association, Washington, 2013).
63. Fusinska-Korpik A, Gacek M. Decision-making regarding social situations in people with intellectual disability at different stages of the decision-making process. Cogn Process. 2024;15:491–501.
64. Seyed-Alipour S, Alaghband-Rad J, Faraji S, Hooshyari Z, Tehranidoost M, Motamed M. Cognitive functioning in adults with autism spectrum disorder. Appl Neuropsychol Adult. 2024 Apr 18:1–8. https://doi.org/10.1080/23279095.2024.2336201. Epub ahead of print.
65. Phillips MS, Bing-Canar H, Shields AN, Cerny B, Chang F, Wisinger AM, et al. Assessment of learning and memory impairments in adults with predominately inattentive versus combined presentation attention-deficit/hyperactivity disorder. Appl Neuropsychol Adult. 2025;32:346–55.
66. Van Rooij D, Anagnostou E, Arango C, Auzias G, Behrmann M, Busatto GF, et al. Cortical and subcortical brain morphometry differences between patients with autism spectrum disorder and healthy individuals across the lifespan: results from the ENIGMA ASD Working Group. AJP. 2018;175:359–69.
67. Khundrakpam BS, Lewis JD, Kostopoulos P, Carbonell F, Evans AC. Cortical thickness abnormalities in autism spectrum disorders through late childhood, adolescence, and adulthood: a large-scale MRI Study. Cerebral Cortex. 2017;27:1721–31.
68. Writing Committee for the Attention-Deficit/Hyperactivity Disorder, Autism Spectrum Disorder, Bipolar Disorder, Major Depressive Disorder, Obsessive-Compulsive Disorder and Schizophrenia ENIGMA Working Groups, et al. Virtual Histology of Cortical Thickness and Shared Neurobiology in 6 Psychiatric Disorders. JAMA Psychiatry. 2021;78:47.
69. Patel Y, Woo A, Shi S, Ayoub R, Shin J, Botta A, et al. Obesity and the cerebral cortex: Underlying neurobiology in mice and humans. Brain Behav Immun. 2024;119:637–47.
70. Mooney MA, Bhatt P, Hermosillo RJM, Ryabinin P, Nikolas M, Faraone SV, et al. Smaller total brain volume but not subcortical structure volume related to common genetic risk for ADHD. Psychol Med. 2021;51:1279–88.
71. Mahmassani HA, Switkowski KM, Scott TM, Johnson EJ, Rifas-Shiman SL, Oken E, et al. Maternal diet quality during pregnancy and child cognition and behavior in a US cohort. Am J Clin Nutr. 2022;115:128–41.
72. Rosario FJ, Kanai Y, Powell TL, Jansson T. Increased placental nutrient transport in a novel mouse model of maternal obesity with fetal overgrowth. Obesity. 2015;23:1663–70.
73. Rivera HM, Christiansen KJ, Sullivan EL. The role of maternal obesity in the risk of neuropsychiatric disorders. Front Neurosci. 2015;9:1–16.
74. Lean SC, Candia AA, Gulacsi E, Lee GCL, Sferruzzi-Perri AN. Obesogenic diet in mice compromises maternal metabolic physiology and lactation ability leading to reductions in neonatal viability. Acta Physiologica. 2022;236:e13861.
75. Bordeleau M, Fernández, de Cossío L, Chakravarty MM, Tremblay M-È. From maternal diet to neurodevelopmental disorders: a story of neuroinflammation. Front Cell Neurosci. 2020;14:612705.
76. Bodden C, Hannan AJ, Reichelt AC. Of 'junk food' and 'brain food': how parental diet influences offspring neurobiology and behaviour. Trends Endocrinol Metab. 2021;32:566–78.
77. Ellulu MS, Patimah I, Khaza'ai H, Rahmat A, Abed Y. Obesity and inflammation: the linking mechanism and the complications. aoms. 2017;4:851–63.
78. Kretschmer T, Schulze-Edinghausen M, Turnwald E-M, Janoschek R, Bae-Gartz I, Zentis P, et al. Effect of maternal obesity in mice on IL-6 levels and placental endothelial cell homeostasis. Nutrients. 2020;12:296.
79. Kim DW, Young SL, Grattan DR, Jasoni CL. Obesity during pregnancy disrupts placental morphology, cell proliferation, and inflammation in a sex-specific manner across gestation in the mouse1. Biology Reprod. 2014;90:1–11.
80. Reiss JD, Peterson LS, Nesamoney SN, Chang AL, Pasca AM, Marić I, et al. Perinatal infection, inflammation, preterm birth, and brain injury: a review with proposals for future investigations. Experimental Neurol. 2022;351:113988.
81. Cheroni C, Caporale N, Testa G. Autism spectrum disorder at the crossroad between genes and environment: contributions, convergences, and interactions in ASD developmental pathophysiology. Mol Autism. 2020;11:69.
82. Zilkha N, Kuperman Y, Kimchi T. High-fat diet exacerbates cognitive rigidity and social deficiency in the BTBR mouse model of autism. Neuroscience. 2017;345:142–54.
83. Wang Y-C, Chen C-H, Yang C-Y, Ling P, Hsu K-S. High-fat diet exacerbates autistic-like restricted repetitive behaviors and social abnormalities in CC2D1A conditional knockout mice. Mol Neurobiol. 2023;60:1331–52.

ACKNOWLEDGEMENTS

This study was supported by the funding from the Canadian Institutes of Health Research (CIHR Project Grant: 175049) and the Ontario Institute for Cancer Research (IA-024) through funding provided by the Government of Ontario to Dr. Nieman. We gratefully acknowledge funding provided by the Canadian Graduate Scholarships – Master's (CGS-M), the Restracomp Master's Scholarship from the Hospital for Sick Children, the Dorothy C. Hodgkin Bursary for Female Graduates, the Ontario Graduate Scholarship, and a graduate fellowship from the University of Toronto awarded to Gail Lee. The authors would like to thank The Centre for Phenogenomics for their assistance and care of animals used in this study.

AUTHOR CONTRIBUTIONS

MP, BN, JL, T-YZ, and JF designed the research study and obtained funding. AW helped design the research study. MP and BN supervised the study. GL, KW, and CC conducted the experiments. Statistical analyses were performed by GL and JY. GL, MP, and BN wrote the manuscript. All authors reviewed and approved the final manuscript.

COMPETING INTERESTS

JAF serves on the Scientific Advisory Board for MRM Health NL and has received consulting/speaker fees from Alphasights, Novozymes, Klaire Labs, Takeda Canada, Rothman, Benson, Hedges Inc, and WebMD. The other authors declare no competing interests.

ETHICS APPROVAL AND CONSENT TO PARTICIPATE

All experiments were performed in accordance with Canadian Council on Animal Care (CCAC) guidelines for the care and use of laboratory animals. All animal care and experimental procedures were approved by The Centre for Phenogenomics Animal Care Committee (AUP 25-0175H). This study did not involve human subjects, and therefore, no ethics approval for human studies, informed consent, or clinical trial registration was required.

ADDITIONAL INFORMATION

Supplementary information The online version contains supplementary material available at https://doi.org/10.1038/s41398-025-03701-z.

Correspondence and requests for materials should be addressed to Gail Lee.

Reprints and permission information is available at http://www.nature.com/reprints

Publisher's note Springer Nature remains neutral with regard to jurisdictional claims in published maps and institutional affiliations.